

# Hidden Interfaces for Ambient Computing: Enabling Interaction in Everyday Materials through High-brightness Visuals on Low-cost Matrix Displays

Alex Olwal  
Google Research  
Mountain View, CA, USA  
olwal@acm.org

Artem Dementyev  
Google Research  
Mountain View, CA, USA  
artemd@google.com



**Figure 1:** *Hidden Interfaces* is designed to be embedded underneath transmissive materials, such as textile, wood veneer, acrylic or one-way mirrors, and appear on-demand for touch-based interaction. Our vision is to enable low-complexity interaction technology that can coexist with everyday materials and aesthetics.

## ABSTRACT

Consumer electronics are increasingly using everyday materials to blend into home environments, often using LEDs or symbol displays under textile meshes. Our surveys ( $n=1499$  and  $n=1501$ ) show interest in interactive graphical displays for hidden interfaces – however, covering such displays significantly limits brightness, material possibilities and legibility.

To overcome these limitations, we leverage parallel rendering to enable ultrabright graphics that can pass through everyday materials. We unlock expressive hidden interfaces using rectilinear graphics on low-cost, mass-produced passive-matrix OLED displays. A technical evaluation across materials, shapes and display techniques, suggests 3.6–40X brightness increase compared to more complex active-matrix OLEDs.

We present interactive prototypes that blend into wood, textile, plastic and mirrored surfaces. Survey feedback ( $n=1572$ ) on our prototypes suggests that smart mirrors are particularly desirable. A lab evaluation ( $n=11$ ) reinforced these findings and allowed us to also characterize performance from hands-on interaction with different content, materials and under varying lighting conditions.

## CCS CONCEPTS

• **Human-centered computing** → Ubiquitous and mobile computing systems and tools; Displays and imagers.

## KEYWORDS

hidden interfaces, parallel rendering, rectilinear, passive-matrix OLED, calm computing, ubiquitous computing, ambient computing

## ACM Reference Format:

Alex Olwal and Artem Dementyev. 2022. Hidden Interfaces for Ambient Computing: Enabling Interaction in Everyday Materials through High-brightness Visuals on Low-cost Matrix Displays. In *CHI Conference on Human Factors in Computing Systems (CHI '22)*, April 29–May 5, 2022, New Orleans, LA, USA. ACM, New York, NY, USA, 20 pages. <https://doi.org/10.1145/3491102.3517674>

## 1 INTRODUCTION

In recent years, we have seen an increased interest in the ability to deliver on the vision of ubiquitous computing. With the proliferation of consumer electronics and smart appliances, homes are beginning to embrace various types of *smart devices*, Internet-connected technology that offer functionality such as music control, voice assistance, and home automation. A graceful integration of these devices requires adaptation to existing aesthetics and user styles. There has thus been an increasing desire to create smart devices and appliances, which can preserve the aesthetics of everyday materials, while providing on-demand access to interaction and digital displays.

Today's smart devices tend to fall into two categories. On the one hand, there are devices with no or minimal displays, where



This work is licensed under a Creative Commons Attribution International 4.0 License.

*CHI '22*, April 29–May 5, 2022, New Orleans, LA, USA  
© 2022 Copyright held by the owner/author(s).  
ACM ISBN 978-1-4503-9157-3/22/04.  
<https://doi.org/10.1145/3491102.3517674>

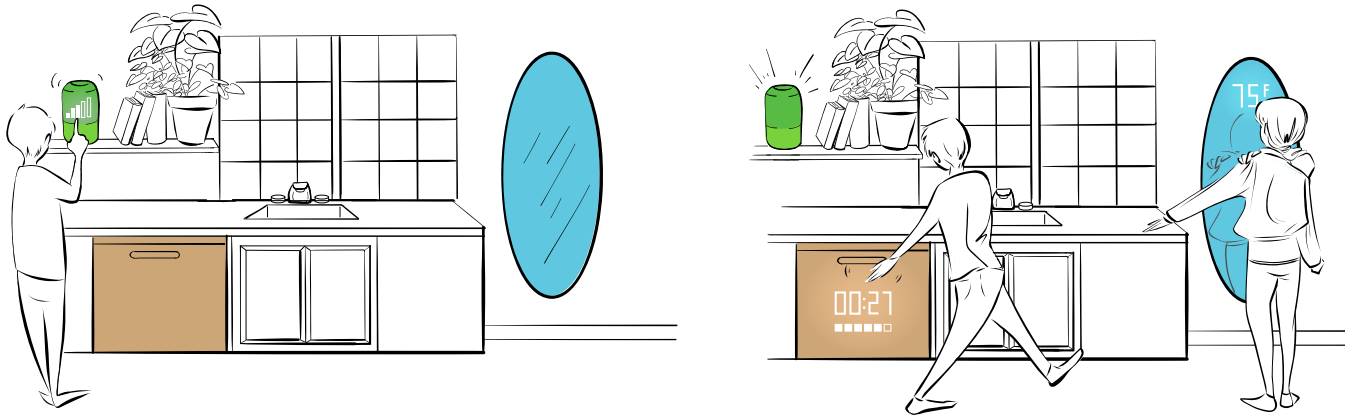


**Figure 2: Concept sketches that illustrate how hidden interfaces could appear and disappear in everyday materials and appliances. From left to right: The speaker’s volume control appears upon touch; The dishwasher displays the remaining time (27 minutes) and the current wash cycle (5/6) when the user waves their hand; The mirror displays the current outdoor temperature (75° Fahrenheit) when it detects a user in front of it.**

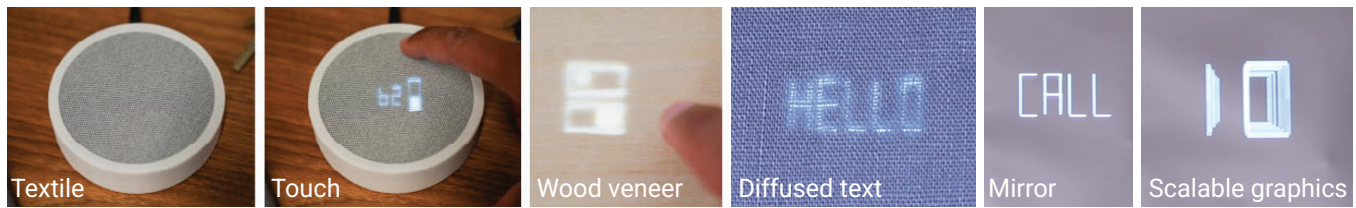


**Figure 3: Parallel rectilinear rendering achieves ultra-bright graphics on low-cost passive-matrix OLED displays. From left to right: Display hidden under textile; Touch-activated controls; Switches under veneer; Typography diffused by textile; Clear text under mirror; Leveraging high-speed rendering of scalable vector graphics for animated 3D effects.**

the main interaction is performed through a mobile app or using speech. On the other hand, there are high-fidelity touch displays, recently often leveraging active-matrix OLED (AMOLED) technology. Their disadvantage is the tension that screens create with everyday materials, and when turned off, black screens become “black holes” that disrupt the physical environment.

To enable expressive displays without these tradeoffs, strategies have been developed to realize displays that can disappear. Partially reflective material has been used to hide displays when not in use in e.g., smart mirrors (e.g., [4, 16]), TV mirrors (e.g., [28, 29]) and smart thermostats [14]. Frosted, translucent materials can hide displays, but absorb and distort light, which limits their use to basic diffuse and dim graphics (e.g., [13]). Today’s brightest displays are expensive and complex as they are optimized for image quality. Rendering strategies for low-cost displays on the other hand, are typically not effective in generating sufficient light to pass through everyday materials. To overcome this limitation, smart speakers are increasingly using textile mesh covers with special-purpose illumination. They employ high-brightness LEDs underneath textile to provide abstract indicators [12], 7-segment displays to show time [32], or to illuminate fixed icons [41]. These special-purpose displays are, however, limited to basic, predefined content. Projectors have also been proposed for on-demand interfaces, but they are less relevant

for our use cases of self-contained smart home devices, since they are not designed to fit into compact and flat form factors. Front projection, on the other hand, might not be practical in everyday home environments due to brightness limitations, occlusion issues and the need for calibration, alignment and distortion correction. Additionally, it is not practical to project onto reflective, specular, or textile mesh surfaces.

Hidden interfaces that can blend into the environment have a unique potential to balance aesthetics and functionality, with new opportunities for ubiquitous computing (See Figure 1). We realized a system that can allow home device controls to appear from underneath textile, wood, plastic and mirrors — and fade out and disappear when not in use, as illustrated in Figure 2. In this work, we advance the potential symbiosis of electronics and everyday environments through user research, interaction technology and technical characterizations.

Specifically, our work focuses on hidden displays that can support interaction with expressive, reconfigurable graphical user interfaces (UIs), expressive scalable vector graphics, and typography (See Figure 3). Our direction is informed by large-scale surveys (n=1499 and n=1502), which show clear interest in such displays and provide insights on participants’ material and content preferences. To enable the required high-brightness visuals to pass through

materials, we leverage efficient parallelized rendering on passive-matrix OLED (PMOLED) displays using rectilinear, axis-aligned lines. We use hardware prototypes to demonstrate UIs that can appear through transmissive materials using low-cost PMOLEDs. By coupling our visual output with capacitive sensing, we enable a series of applications across four types of everyday materials. To validate the advantages of the approach, we conducted a technical evaluation using seven material conditions, four displays, and content consisting of simple shapes, text and UI elements. We also solicited feedback on six implemented use cases in an evaluative large-scale survey (n=1572). Finally, we conducted a user study with 11 participants that provides quantitative and qualitative feedback on interactions with our display under different lighting conditions, materials and applications.

## 1.1 Contributions

The contributions of this work are:

- **Foundational large-scale surveys with 1499 and 1502 participants**, which provide insights on who may be interested in hidden interfaces, and the most promising materials and content types.
- **Hidden Interfaces hardware and UIs** that implement on-demand interaction using high-brightness, parallel rendering of rectilinear elements on low-cost PMOLED displays. We demonstrate scalable graphical UI elements and typography with fluid animation enabled by high-speed rendering.
- **Technical evaluation** that characterizes the technique's performance in seven material conditions, comparing it to three baselines (scanline rendering and two high-quality AMOLED displays), with basic primitives, as well as a selection of representative UI elements and text. Our analysis suggests that our method can achieve more than 3.6–40X increase in brightness for rectilinear graphics on most transmissive materials for these types of content.
- **Evaluative large-scale survey with 1572 participants** on the desirability of our implemented hidden interface use cases.
- **Evaluative lab study with 11 participants** that provides feedback from hands-on experiences with our prototypes. We report results from content being viewed under different ambient lighting, performance measured in a targeting task, and qualitative feedback on concept, use cases and materials.

## 2 RELATED WORK

### 2.1 Hidden textile displays

Hidden displays are often explored in the context of textiles so that they can be discreetly embedded in clothing, for example, using braiding [25], knitting [26], and weaving [5] to enable the integration of flexible, emissive optical fibers with textile fibers, using manual techniques or through programmable industrial machines. Such displays can appear and disappear while minimally impacting the appearance of the fabric. Discrete LEDs have also been manually sewn into textiles with conductive thread [3]. Arranging discrete LEDs into graphical display matrices is possible, but ineffective and limited to low pixel densities, greatly constraining the

possible expressivity. To add graphical display capabilities, other approaches include liquid crystal ink [38], thermochromic ink [7, 27], and electroluminescent materials [15]. These techniques have other challenges, such as no or low light emission, slow refresh rates, and, most importantly, limited scalability of the fabrication methods. Additionally, they usually do not inherently provide a mechanism to hide the display when not in use. Our technique provides an expressive graphical display, which can appear/disappear on demand with fast refresh rates, and we leverage widely available and low-cost PMOLED technology. While textile display research is typically focused on material integration, ambient displays also require low-cost, low-complexity and always-on capabilities.

### 2.2 Ambient displays

Ideas and research around ambient displays have been popular in ubiquitous computing [21, 37]. E-ink has been integrated into wearables, such as clothing [8] and nails [9], and been powered wirelessly using Near-Field Communication (NFC) [6]. E-ink's main disadvantage is a slow refresh rate and high power consumption during screen updates, making it less suitable for real-time interface and interactions.

Living Wood [18] created an inspiring alphanumeric segmented display underneath wood, but resolution and scalability is limited by complex individual wiring to each LED. The limited expressivity of the segmented display is also amplified by perceptual risks [35].

Ambient displays can also take non-graphical forms, such as embedding custom-designed displays in everyday objects or walls, using screen printing of electroluminescent materials [24]. Other ambient displays follow the philosophy of tangible interfaces [17] to communicate using movement or shape change [40]. The major disadvantage of such displays is their limited expressivity. Even in our proof-of-concept implementation with a 128×96 resolution, we have more than 12 000 individually controllable LEDs in a dense arrangement. It is, however, critical to balance complexity, expressivity and scalability in ambient displays to match intended use.

### 2.3 Optimizing display performance for specific applications

While many applications can leverage generic display configurations and drivers, researchers continue to optimize performance for specific applications through innovative software and hardware. Many rendering techniques focus on environmental light correction [23, 33] or image quality, such as resolution, contrast, brightness, and depth of field. Computational techniques include using image decomposition to improve image quality [30], whereas custom hardware allowed multi-layer LCDs [19] to increase resolution and depth of field, or enable high dynamic range (HDR) through projected modulated light [2]. Custom displays are, however, expensive to produce at scale — thus, there are advantages in leveraging inexpensive off-the-shelf displays. Rendering techniques have also been used to reduce OLED power consumption, by selectively dimming parts of the screen where the user is not looking [39]. Inspired by this research, we use a parallel rendering pipeline that is particularly suitable for high-brightness rendering of rectilinear UI primitives on widely available and low-cost display technology.

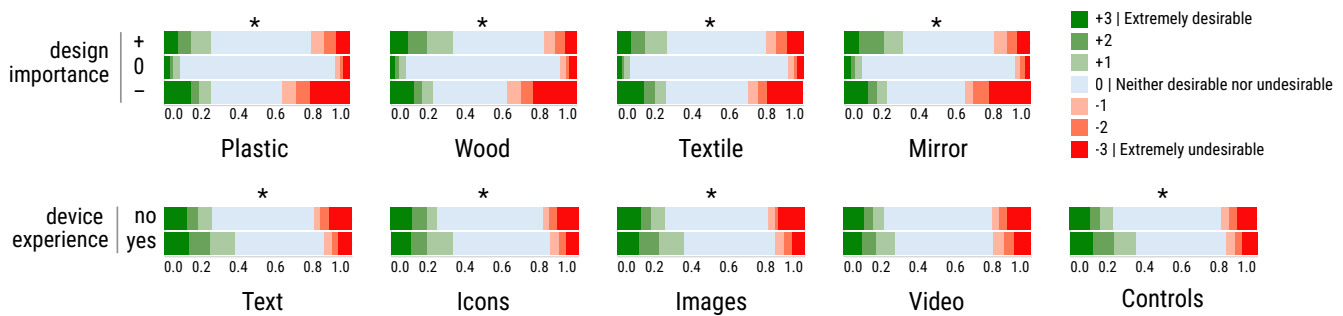


**Figure 4: Desirability rankings for hidden interface materials and content. *Top:* Material preferences for participants who feel that it is important (+), unimportant (-) or neither (0) that smart device aesthetics match the user’s home (n=1499). *Bottom:* Content preferences for participants who have (yes) and have no (no) experience using home devices (n=1502).**

### 3 FOUNDATIONAL LARGE-SCALE SURVEYS WITH 1499 AND 1502 PARTICIPANTS

To learn about the potential for hidden interfaces, we decided to leverage large-scale surveys to get a broad representation of the general population. Our goal was to understand the desirability of hidden interfaces, various cover materials and content to display – and how attitudes might vary based on home device usage and interest in style and aesthetics.

#### 3.1 Participants

We used Google Surveys [11] to deploy two surveys (due to limitation of ten questions per survey) to the general population in the US of all ages and gender, since that was the largest English-speaking population that we could target with the tool to get broad representation (“*Internet users reading content on a network of web-publisher sites using Google Opinion Rewards for Publishers*”) [11]. Furthermore, the US has the highest penetration rate for smart homes [34]. Survey 1 focused on attitudes towards specific materials that the device could be hidden under, whereas Survey 2 focused on attitudes towards the types of content that such hidden devices could display. For the 1499 complete responses in Survey 1, the platform reported that 34% were women, 42% men, and 24% unknown, across all age ranges (4%: 18–24, 13%: 25–34, 13%: 35–44, 14%: 45–54, 16%: 55–64, 16%: 65+, and 24% unknown). For the 1502 complete responses from Survey 2, 30% were women, 44% men, and 26% unknown, across all age ranges (4%: 18–24, 11%: 25–34, 12%: 35–44, 14%: 45–54, 17%: 55–64, 16%: 65+, and 26% unknown).

#### 3.2 Results

We summarize the main findings in this section, but the detailed statistical analysis is provided in Appendix A.

*Specific materials. Desirability for devices hidden under plastic, wood, mirror or textile (n=1499).* The results suggest that people who ranked design importance high also rated wood and mirror materials significantly higher than others. See Figure 4, top.

*Specific content. Desirability for different content (n=1502).* The results suggest that there was a statistically significant difference in content type ratings for the whole population and between groups with different home devices usage. Overall, text was ranked highest. Text and image content were also both significantly higher rated

than video. Additionally, people who had used home devices rated text, controls and images significantly higher than others. See Figure 4, bottom.

#### 3.3 Discussion

*Perceived importance of design led to higher preference for wood and mirror materials.* Today’s consumer devices that use displays underneath material mostly leverage textile meshes or plastic, with mirrored surfaces being less common. While we did not see an effect for our general population or based on device experience, our analysis did show that design preference influences how desirable people find different materials. Especially, we identified that this group more than others favored wood and mirror materials, as shown in Figure 4, top. This insight suggests an opportunity to explore displays that could penetrate wood surfaces, while also being compatible with plastic, textile and mirrored surfaces.

*Experience with home devices led to stronger preference for text, controls and images.* Home devices span a wide range of display capabilities, from basic digital time displays to high-definition tablet-sized screens. Our analysis helps inform the types of content to support in hidden interfaces by showing that people who had used devices rated text, UI controls and images higher, and that video was the least desirable content. See Figure 4, bottom.

## 4 EFFICIENT, HIGH-BRIGHTNESS RENDERING FOR AMBIENT DEVICES

The large-scale surveys suggested potential for hidden displays that present simple graphics and text. In this section, we discuss how content-aware rendering enables low-cost and widely available matrix displays to gain the significant brightness needed to penetrate everyday materials, unlocking their potential for use as cost-effective hidden interfaces.

### 4.1 Popular special-purpose displays do not emit enough light to penetrate materials

Products select displays based on both application needs and trade-offs between cost and complexity. Thus, we continue to see products that use E-ink for E-book readers, LEDs for oven timers, and

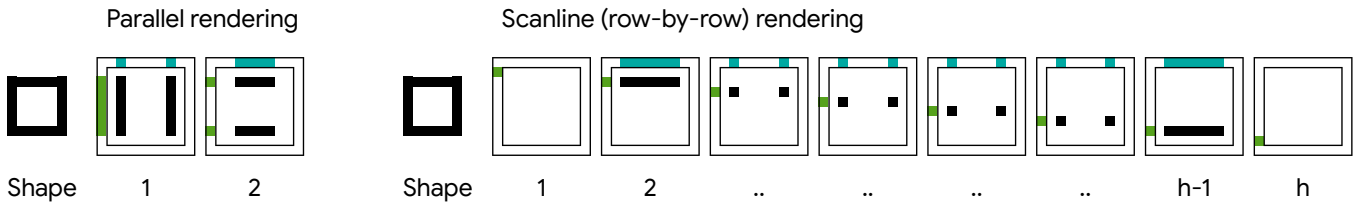


**Figure 5: Parallel rendering activates multiple rows simultaneously to take advantage of redundancies in rectilinear graphics, which can greatly reduce the number of frames needed to render contents. The Scanline content-agnostic rendering processes each row, which limits the brightness since at most one row can be illuminated at a time.**

**Table 1: Simple rectilinear primitives require only 1 or 2 operations with parallel rendering, compared to the scanline technique, which requires iterations through all rows that make up the display height ( $h$ ).**

Primitive	Parallel rendering	Scanline (row-by-row)
Solid rectangle	1 operation	$h$ operations (all shapes)
Hollow rectangle	2 operations (horizontal + vertical lines)	
Vertical line	1 operation	
Horizontal line	1 operation	

LCDs for microwaves. While many of those technologies are cost-effective at scale, none of them have the emissive capabilities to display images from underneath materials.

## 4.2 Cost and complexity of AMOLEDs is prohibitive for ambient devices

While many of today's consumer devices employ AMOLED displays, active electronics greatly increase complexity and cost. AMOLEDs are therefore mainly used in high-end devices, such as smartphones, tablets and premium smartwatches, as their cost and manufacturing complexity is prohibitive for ubiquitous computing devices. While the cost and availability of premium AMOLED displays will improve over time, they are still not ideal for every application or product.

## 4.3 PMOLEDs low brightness is the result of content-agnostic scanline rendering

AMOLEDs achieve high-quality, flicker-free and bright graphics through dedicated memory, which maintains per-pixel state.

PMOLEDs, however, are based on a simple design without per-pixel memory, which greatly reduces manufacturing costs and complexity. Thus, they continue to be used in basic devices where AMOLEDs are too advanced, as PMOLEDs are a great match for small, low-complexity UIs with limited resolution. The disadvantage of PMOLEDs is that they require active display driver circuitry that runs an update loop to select columns and power rows, controlling how current flows through and illuminates specific pixels. To display general-purpose content, existing drivers inspect the framebuffer using the scanline technique (row-by-row), and select which columns to activate for each row. For each display frame, they thus need to iterate through all rows for the height of the display. This process results in only one row of pixels turned on at a time, which limits the instantaneous display brightness to the luminance of 1 row of pixels (width  $\times$  per-pixel luminance). The vertical temporal multiplexing can also introduce flicker since all

rows except one are always turned off. See Figure 5, "Scanline" (right).

## 4.4 Parallel rendering can boost PMOLED brightness by several orders of magnitude

However, similarly to how multiple columns can be selected, we can also simultaneously enable multiple rows. The parallel powering of multiple rows replicates the column pattern across the rows, with the potential for more light output and higher frame rate. This technique is most effective when it is applied to rectilinear, axis-aligned geometry, such as rectangles, where there is inherent redundancy of content across rows. A significant increase in performance is thus possible if we can use rectilinear primitives as input to the display driver, rather than framebuffer pixels. For example, Figure 5 shows how a rectangle outline can be rendered with just two operations, when parallel rendering can activate all similar rows. The corresponding scanline version will need a frame for each row, resulting in as many operations as there are rows –  $height(display)$  operations.

The architecture also supports unique brightness levels in each operation through variation of the voltage differential between rows and columns. Thus, we can control per-pixel brightness by providing unique values in each activated column, and unique values in each activated row. For example, interpolating from  $[0..255]$  for a column vector, and  $[0..255]$  for a row vector would render a gradient fill from 0 (top, left) to full brightness (bottom, right), in a single operation. Figure 3 shows a practical example of how slide switches under veneer are rendered dim when off (top) and brighter when on (bottom).

The technique is not strictly limited to lines and rectangles, even if that is where we see the most dramatic performance increase. Rounded shapes can be achieved by omitting corner pixels, requiring 1 additional operation for filled rectangles, but no additional operations for hollow rectangles. We can also add antialiasing pixels for smoothing, where we render four corner pixels in a single

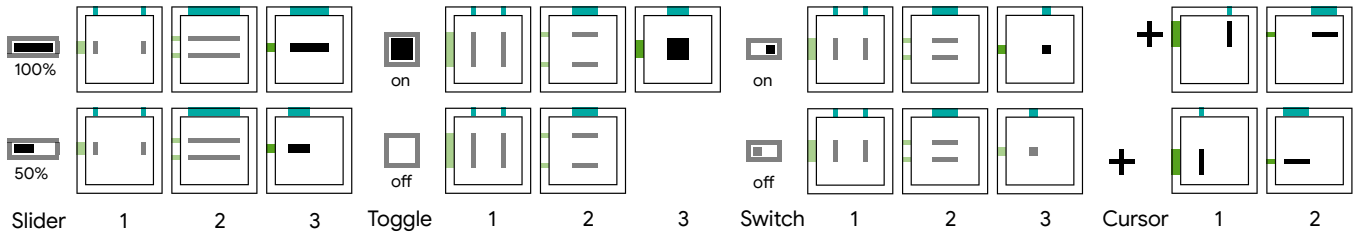


**Figure 6: Slider, toggle, switch and cursor. Using primitives, we compose basic UI elements for continuous or binary input.**

operation. Diagonal lines and circles benefit the least from our approach, given that their content has little redundancy across rows. Worst case is when we need a unique row/column combination for each pixel in a diagonal line across the width/height of the display, which would result in the same performance as the scanline algorithm. Circles could, however, leverage their symmetry when decomposed into vertical and horizontal lines to achieve at least 2X the performance of the scanline algorithm.

This work leverages the temporal and spatial advantages of parallel rendering for significantly brighter graphics thanks to both the drastic speed-up and the ability to illuminate larger areas of the display in each frame, compared to a single row for scanline rendering.

## 5 SCALABLE RECTILINEAR UI PRIMITIVES AND CONTROLS

The survey results suggest a preference for UI elements and text over more complex content (e.g., video), which supports our emphasis on rectilinear graphics and UI-focused application scenarios. To fully take advantage of the parallel rendering of multiple rows, we designed a system around rectilinear graphics that can be rendered efficiently based on the redundancy across rows and columns. The designer can thus balance desired display brightness with the number of on-screen elements, and further leverage aligned graphics to exploit redundancies. Rectilinear redundancies also allow arbitrary stroke thickness and effects. (See Figure 3). Graphics can be scaled, stretched and moved freely on the canvas from frame-to-frame, enabling fluid animations and pseudo-3D effects. The system is designed for a small set of minimal UI elements to enable occasional and sporadic interactions with on-demand interfaces and is not suitable nor intended to be a complete UI framework with advanced compositions. We envision that each interface can provide different basic controls, such as light switches, volume controls and thermostats — but only showing one at a time.

### 5.1 Basic primitives: rectangles and lines

Rectangles and lines form our basic elements, which we render with just 1 or 2 operations (See Table 1). For these primitives the speed-up is  $(0.5 \text{ to } 1) \times$  the display height ( $h$ ) compared to the scanline approach. On our  $128 \times 96$ -pixel display, a hollow rectangle and a filled rectangle can thus appear 48X or 96X brighter, respectively. We can further compose rectangles and lines to form a basic set of user interface controls for parallel rendering, as shown in Figure 6.

### 5.2 Sliders: continuous parameters

The vertical/horizontal slider is a widely used UI-element. To control and visualize continuous parameters, like audio volume, we combine a darker hollow rectangle (outline), partially filled with a bright solid rectangle, as shown in Figure 7, which also shows how we can leverage the ability to use different brightness levels across operations. Per Table 1, composing a dark hollow rectangle and a solid fill requires 3 operations. We support arbitrary stroke thickness, since that just adds redundant lines, which we can render in the same operation.

Additionally, we can use multiple bars to visualize, e.g., audio spectrum during music playback or to control multiple parameters, such as RGB/HSV color for a smart lightbulb. We can render  $n$  horizontal sliders using 3 operations if they are all on a single row, or using  $2+n$  operations if they are all aligned vertically. The aligned outlines are rendered in parallel using 2 operations. For sliders on a single row, we can render all unique values in 1 operation, whereas vertically aligned sliders require 1 operation for each.

### 5.3 Selection controls: toggles, radio buttons, and switches

Figure 7 shows our implementation of *Toggle* and *Switch*, two common selection controls. The toggle can be used for both checkboxes (multi-choice) and radio buttons (exclusive selection). We render it with a dark hollow rectangle when not selected (2 operations), and add a bright filled rectangle when selected (3 operations). For our switch, we use a dark outline and fill it with a dark rectangle to the left (off), or with a bright rectangle to the right (on).

### 5.4 Cursor: 2D selections

A 2D cursor could be useful for certain selections and controls. For example, for controlling the color of smart lights, we could use the Y-axis for brightness, and X-axis for hue. To support such interactions, we use a crosshair, which can be rendered in 2 operations (horizontal line + vertical line).

### 5.5 Scalable typography: animations, effects and interaction with segmented characters

We enable parallel rendering of interactive text and digits in hidden interfaces by segmenting characters into shared rectilinear components. We maximize the reuse of a small number of unique row/column combinations such that the full character set can be composed with as few operations as possible. We are, however, not limited to specific resolutions or positions given that it is a

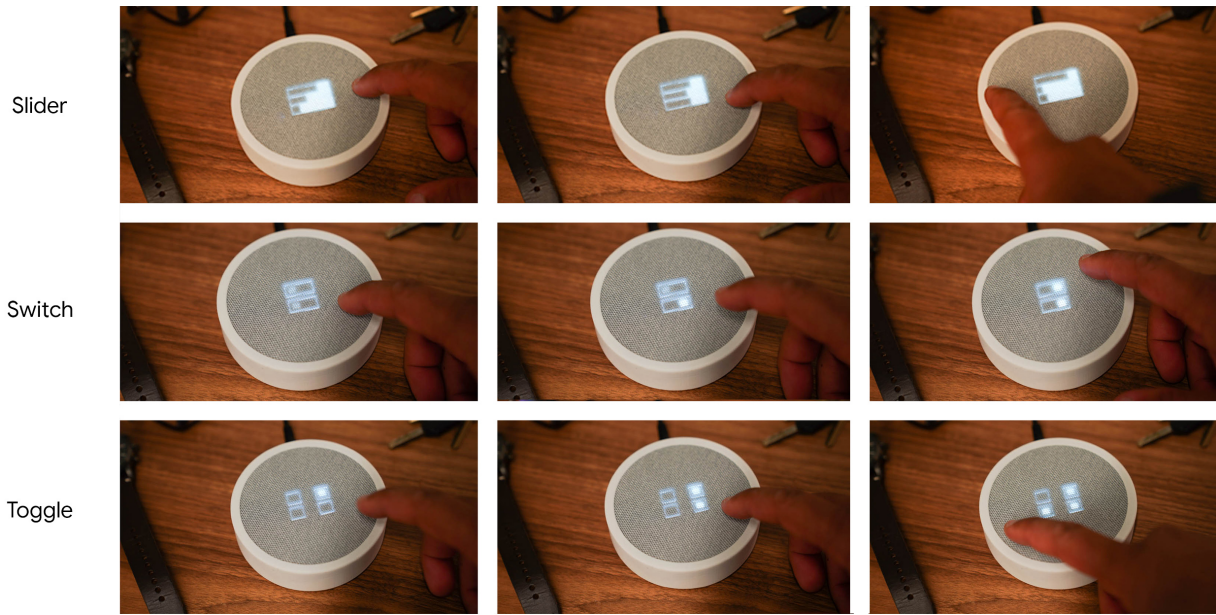


**Figure 7: UI elements through textile.** *Top:* Slider. The sliders move left when touching the capacitive touch sensor on the left and vice versa. The sliders are composed of a dark hollow rectangle and a bright solid rectangle. *Center:* Switch. The switch will toggle on/off when touched nearby. It renders dark when turned off and bright when turned on. *Bottom:* Toggle. Selection boxes will toggle between filled/hollow (on/off) when the closest electrode is tapped.

matrix display. There are many possible strategies to implement characters using segments, and to demonstrate the versatility of the matrix display, we implement 7-segment characters to facilitate comparison with popular 7-segment LED displays, which have fixed positions and resolution. Our implementation is a proof-of-concept, which omits characters with diagonal strokes (e.g., "k", "v", "x"), but it would be straightforward to extend the font with additional segments that trade brightness for resolution with additional operations.

*5.5.1 Optimized rendering of 7-segment characters.* Individual 7-segment characters require  $\leq 3$  operations, whereas a string of any length requires  $\leq 5$  operations due to the redundancies across rows and columns. Figure 8 shows how character sequences have  $\leq 3$  unique groups of horizontal strokes and  $\leq 2$  unique groups of vertical strokes. Figure 9 shows a thermostat control with digits and bar graph.

*5.5.2 Scalable typography.* There is no added cost in introducing or modifying segments as long as they align with existing groups.

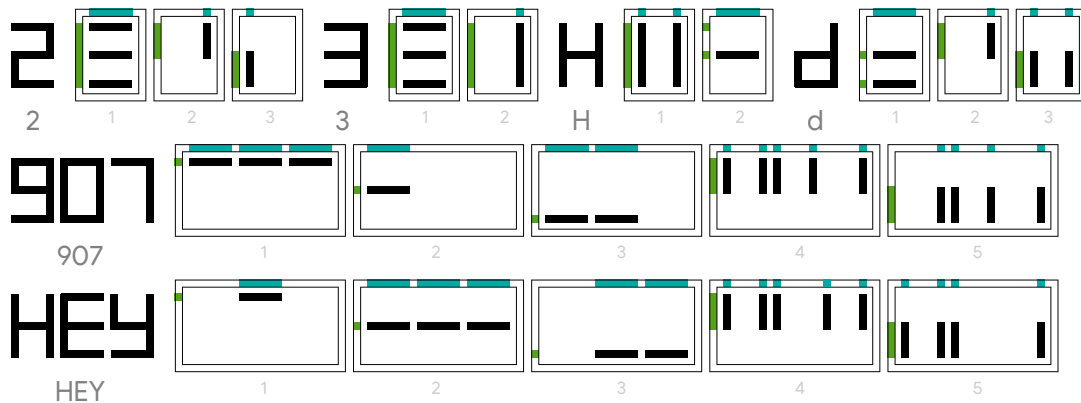


**Figure 8: Scalable typography: 7-segment characters.** Individual characters can be rendered in 1-3 operations. Strings of arbitrary length require at most 5 operations, since there can only be 3 unique groups of horizontal strokes and 2 unique groups of vertical strokes. See "907"/"HEY", operations 1-3 and 4-5.



**Figure 9: Thermostat control on veneer.** The current temperature is displayed with digits, as well as mapped on a bar graph. The temperature can be adjusted by touching the top or bottom.

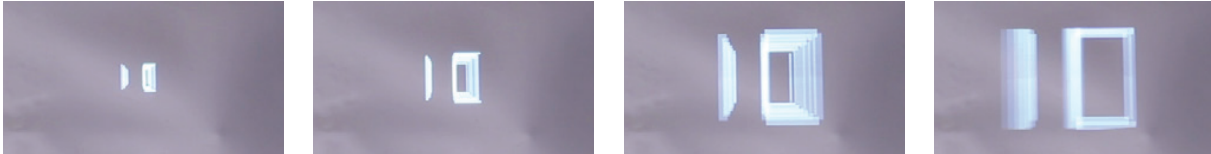


**Figure 10: Animating typography.** Per-frame control of rendering parameters enables 2.5D effects. Here, the number "10" is shown with scale, brightness and strokeweight increasing with "proximity" to the viewer. In contrast to fixed 7-segment LEDs, our high-speed matrix display allows the font to be smoothly animated, enabling the text to scroll, bounce, scale, or zoom.

We can therefore dynamically vary strokeweight to make thinner/thicker characters, change font size or adjust aspect ratio, e.g., to fit more characters onto the screen. Such changes can be applied on a per-frame basis to animate text properties in real-time. This flexibility is a major advantage compared to traditional 7-segment displays where the segments are in a fixed size, shape and position.

**5.5.3 Animations, Effects and Interaction.** The per-frame-control of font properties coupled with the high frame rate of the display enables very fluid animations. These capabilities greatly expand the expressivity of the rectilinear graphics, far beyond what is possible on fixed 7-segment LED displays. We implemented three effects to illustrate this expressivity:

- (1) **1D Scrolling text.** Scrolling ticker that smoothly animates text going from right to left for showing longer messages. Users can interactively control the speed. A fixed 7-segment LED display would have to shift characters in large discrete steps (the width of one digit at a time), which would interfere with the perception of continuity.
- (2) **Text with 2D motion.** Clock display that users can position in 2D using touch interaction – by scaling the font size, users can choose between larger digits showing hours and minutes, or smaller digits that include seconds.
- (3) **Text with 2.5D motion.** By leveraging per-frame changes to scale, brightness and strokeweight, we realized a zooming effect in our countdown display where numbers sequentially "fly" out towards the user. (Figure 10).

## 6 IMPLEMENTATION

In our proof-of-concept implementation, we leverage a PMOLED display (Truly) with  $128 \times 96$  resolution that has all rows and columns broken out to a flexible header. Unlike PMOLED displays in products, it has no driver chip, instead all row/column drivers are routed to a connector for direct access. We use a custom PCB with fourteen 16-channel Digital-to-Analog Converters (DACs) to directly

interface the 224 lines ( $14 \text{ DACs} \times 16 \text{ channels} = 224 \text{ channels} = 128 \text{ columns} + 96 \text{ rows}$ ) from a Raspberry Pi 3 A+ over SPI. Software creates each frame by writing row and column voltages to a frame-buffer, which are then clocked out to the DACs (Analog Devices LTC2668).

For touch interaction, we built a ring-shaped PCB surrounding the display with 12 electrodes arranged in arc segments. The electrodes are connected to a capacitive proximity touch sensor controller (NXP MPR121), which is interfaced over  $I^2C$  from the Raspberry Pi. Our software is written in Python. See Figure 9 for an interactive thermostat with scalable text, graphical slider and touch-based interaction.

A 3D-printed cylindrical enclosure encapsulates all components, except the power supply. The enclosure is designed to also hold in place different materials to allow characterization. Flexible materials, such as textile, can be stretched over it, whereas rigid materials are cut into circular discs. See Figure 11.

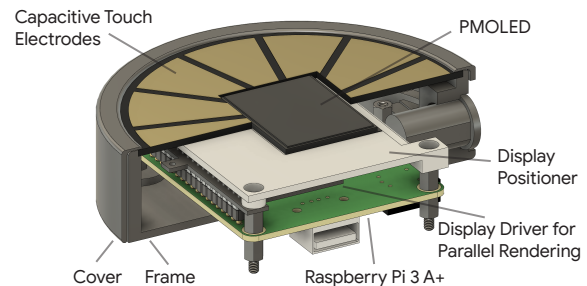


**Figure 11: The physical prototype is designed as a compact stack of a Raspberry Pi 3 A+ single-board computer, custom PCB with analog DACs, custom PMOLED, and a ring-shaped PCB with electrodes for capacitive touch.**

## 7 TECHNICAL EVALUATION

To evaluate our hidden interfaces capabilities we characterize display performance through four common transmissive materials and compare with traditional scanline rendering on PMOLED and two modern AMOLED displays.

### 7.1 Experimental setup for brightness characterization through materials

To assess how well our approach enables hidden interfaces in traditional materials, we performed a technical characterization across different materials with transmissive properties to quantify the effects on brightness. We placed the display flush behind the transmissive materials and measured brightness on the other side with a light meter (Speedmaster L-958D-U, Sekonic) 10 mm away from the display. We measured brightness in lux (lx), a unit that indicates light intensity as perceived by the human eye. We report the maximum value from five measurements. Before each measurement, we obtained the baseline lux value with the display turned off to ensure consistent capture. The environmental light was kept dim to provide a mean of 0.2 lx, which is slightly above the light meter’s minimum sensitivity. The displays were powered by a benchtop power supply (SPD1168X, Siglent), which was also used to measure the current consumption using its integrated meter.

**7.1.1 Material conditions.** We measured the brightness in seven conditions — with no material and with six everyday materials (as

shown in Figure 12), where the choice of materials was informed by the large-scale survey results and common use in home environments:

- (1) **No cover.** (baseline)
- (2) **Acrylic, white translucent** (AC915-W12L24Q4, Plastic-Craft Products). 1.6 mm thickness.
- (3) **PETG, clear** (SainSmart PRO-3). 1 mm thickness. 3D-printed (FDM: MK3S, Prusa), 15% fill and 0.2 mm layers.
- (4) **Wood veneer** (SCV-20-MXDOM&EXOTIC, Sauers). 0.5 mm thickness.
- (5) **Mirror: one-way vinyl window film with a mirror finish** (SV006901000, HIDBEA). 0.2 mm thickness.
- (6) **Basswood sheet** (111222333, Qj-solar). 1.6 mm thickness.
- (7) **Textile: Gray Linen Fabric** (Dekothe) 0.4 mm thickness. Textile mesh, similar to common smart speaker material.

**7.1.2 Apparatus.** We used three baselines to contextualize the performance of the parallel rendering on our PMOLED. Our first baseline is scanline rendering on the same PMOLED panel. We also compare against two AMOLED displays since performance can vary with size. Baseline 2 is a small, 1.4" modern AMOLED display (TOP139AMOLED01.0, Wisecoco), designed for smartwatch use. It was chosen as it is close in size to our PMOLED (27×21 mm) with its 35.3 mm radius and 400×400 resolution. Baseline 3 is a larger 5.5" (140 mm) AMOLED display (16103, Waveshare) with 1920×1080 resolution. Both displays are driven by an HDMI driver, connected to a PC. The displays are attached to an evaluation board

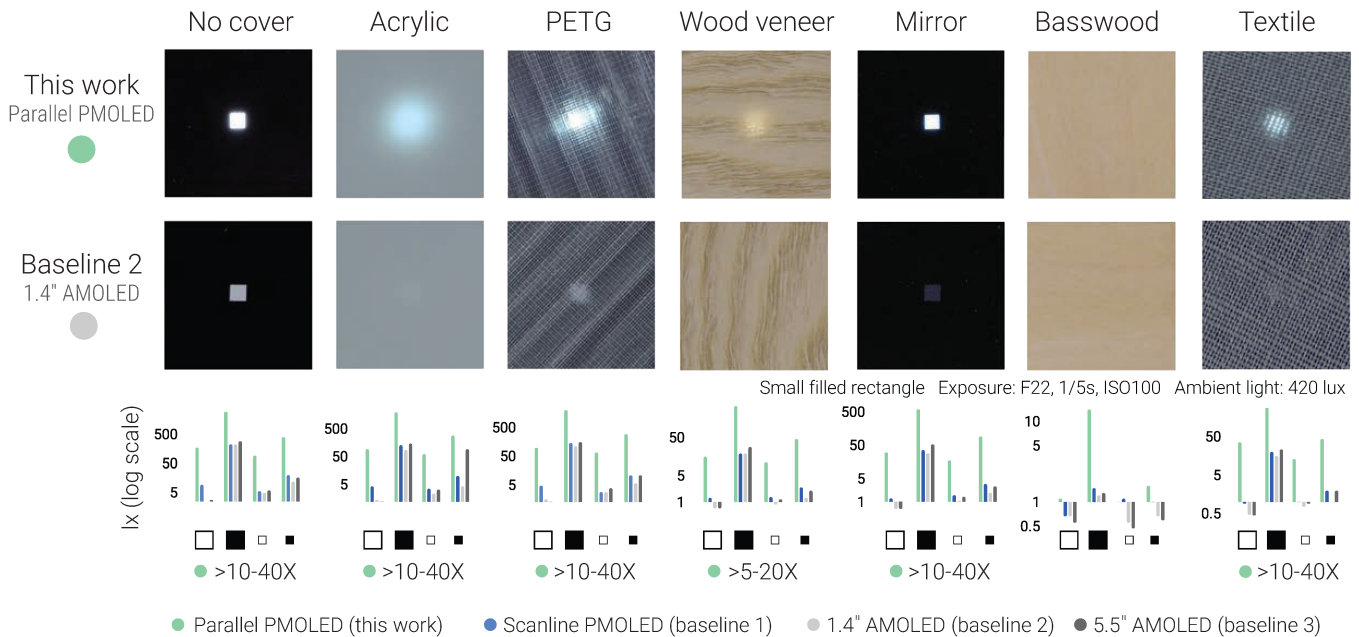


**Figure 12: Top:** An example showing the performance difference between parallel rendering on the PMOLED (this work) and a similarly sized modern AMOLED (baseline 2), when displaying a small filled rectangle in seven material conditions. The displays are covered by the materials used in our evaluation to illustrate the resulting brightness, diffusion and absorption. **Bottom:** For each material, we show logarithmic plots comparing the parallel PMOLED rendering (this work) with the three baselines for the four shapes (small/large×filled/unfilled rectangles). The logarithmic plots reveal how our technique achieves many times the brightness (>5-40X) of the baselines for most materials and shapes.

**Table 2: An overview of the measured brightness values (lx) across four types of rectangles and seven material conditions using PMOLED parallel (this work) and the three baselines: PMOLED scanline (baseline 1), and a small (baseline 2) and large (baseline 3) state-of-the-art AMOLED display. Cells are color-coded if the brightness is >5X, >10X, >20X or >40X dimmer than our technique. PMOLED parallel is brighter across all material and content, in most cases >5-40X brighter than the baselines, making it a promising approach to enable cost-effective and expressive hidden interfaces.**

All values in lx	□ Large unfilled rectangle				■ Large filled rectangle				□ Small unfilled rectangle				■ Small filled rectangle			
	Parallel PMOLED	Scanline PMOLED	1.4" AMOLED	5.5" AMOLED	Parallel PMOLED	Scanline PMOLED	1.4" AMOLED	5.5" AMOLED	Parallel PMOLED	Scanline PMOLED	1.4" AMOLED	5.5" AMOLED	Parallel PMOLED	Scanline PMOLED	1.4" AMOLED	5.5" AMOLED
<b>No cover</b>	170.00	9.30	2.50	2.80	3 000.00	230.00	230.00	280.00	90.00	5.40	5.00	6.00	400.00	20.00	12.00	16.00
<b>Acrylic</b>	90.00	4.40	1.40	1.20	2 000.00	130.00	86.00	150.00	60.00	3.50	2.30	3.30	280.00	10.00	4.40	9.00
<b>PETG</b>	100.00	4.70	1.60	1.30	2 000.00	140.00	110.00	150.00	65.00	2.90	2.90	3.80	300.00	11.00	5.70	11.00
<b>Wood Veneer</b>	16.00	1.30	0.70	0.70	340.00	19.00	19.00	28.00	11.00	1.40	0.90	1.20	46.00	2.50	1.30	2.00
<b>Mirror</b>	30.00	1.30	0.63	0.63	600.00	35.00	28.00	53.00	17.00	1.60	1.10	1.40	90.00	3.50	1.90	3.00
<b>Basswood</b>	1.10	0.67	0.67	0.55	14.00	1.50	1.20	1.30	1.00	1.10	0.55	0.47	1.60	1.00	0.67	0.60
<b>Textile</b>	35.00	0.90	0.47	0.45	280.00	20.00	16.00	23.00	13.00	1.00	0.77	0.90	43.00	2.00	1.00	2.00

Measured lux in comparison to **Parallel PMOLED (this work)**

> 5X dimmer
> 10X dimmer
> 20X dimmer
> 40X dimmer

to allow current measurements and they provide direct interface access without requiring an operating system. We used white color for the rendered contents and kept the other pixels black.

## 7.2 Evaluation 1: rectangle primitives

We first performed our measurements using four variants of the shapes used for our rectilinear UI elements: Small 3×3 mm filled (1) and unfilled (2) rectangles, large 15×15 mm filled (3), and unfilled (4) rectangles. The unfilled rectangles had a 0.15 mm line thickness.

The parallel rendering was brighter than the three baselines (PМОLED scanline and two AMOLED displays) for all materials and across all shapes, as shown in Figure 12 and Table 2. The parallel rendering was typically ≥10X brighter for all the materials, except for the 1.5 mm basswood sheet since it blocked most of the light for all techniques, even if we observe a 5–10X advantage for the large filled rectangle. The difference was more significant with the thinner 0.5 mm wood veneer with ≥5X the brightness compared to the baselines. As the large-scale surveys indicated a preference for wood and mirror materials, these results are encouraging since our

technique provides a significant brightness boost for both wood veneer (5–20X) and mirror (10–40X).

Figure 12 shows an example of how brightness, absorption, and diffusion varies across the different materials for parallel rendering on the PMOLED, and how it compares to a similarly sized AMOLED display. The PMOLED has a pixel density of 6.4 px/mm, which is quite a bit lower than the AMOLEDs — 11.3 px/mm for the small (baseline 2) and 15.9 px/mm for the large display (baseline 3). To ensure consistent brightness comparisons across shapes, we illuminate the same area on each display, lighting up more pixels for the more dense displays.

The lux values observed for the large filled rectangle suggest that our display can also perform well in sunlight, since outdoor displays need to have a brightness of 1570+ lx (500+ nits) [22]. As shown in Table 2, the large filled rectangle achieved 2000 lx for PETG (FDM 3D-printed) and acrylic. Figure 13 shows how the same content under wood veneer is affected by varying ambient brightness, comparing our parallel PMOLED rendering with the

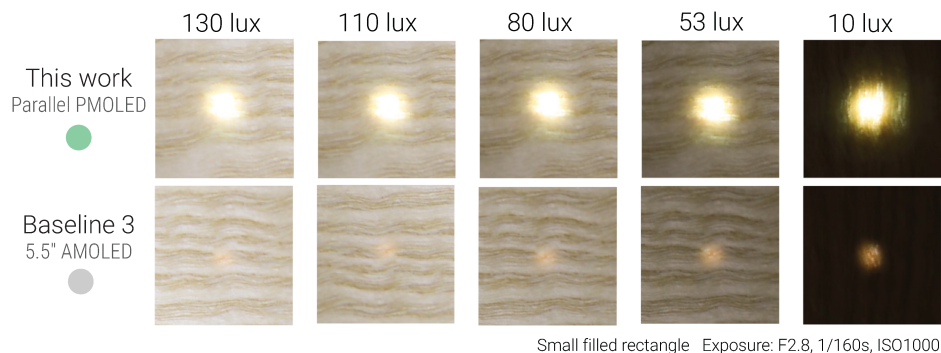


**Figure 13: Display performance under different ambient lighting conditions. This example varies the ambient light from 130 lux (brightest) to 10 lux (darkest) to illustrate the effect on a rendered 3 mm<sup>2</sup> rectangle under wood veneer. *Top*: Parallel rendering on PMOLED (this work). *Bottom*: Same content displayed using the 5.5" AMOLED (baseline 3), which in our lab measurements was >20X dimmer.**

large 5.5" AMOLED (baseline 3). The differences match our lab measurements of >20X higher brightness for the parallel PMOLED.

**7.2.1 Power consumption.** While power consumption might not be critical for wall-powered home devices, it is an essential consideration for battery-powered scenarios. The power varied widely based on content, so we report current consumption while displaying the large filled rectangle. For each measurement, we subtracted the current consumption of the display driver and the Raspberry Pi 3A+. On the PMOLED, we measured 227 mA and 253 mA current consumption for scanline and parallel rendering, respectively. The 11% difference suggests that our approach does not significantly increase energy consumption, while providing >1.5–20X brighter visuals compared to scanline on PMOLED. The small and large AMOLEDs consumed 79 mA and 174 mA, respectively. While our technique had a 1.5–3X increase in energy consumption, it is still more efficient, given the significantly brighter visuals (often 10–20X). We do, however, believe that more optimized display drivers could be beneficial to help reduce power consumption.

### 7.3 Evaluation 2: representative UI elements — number, sliders, toggles, and text string

To contextualize the findings from our technical characterization with more realistic content, we also evaluated a selection of UIs that could be rendered with 3–5 operations.

- (1) Number "2" to represent the worst-case scenario for rendering a single 7-segment character, since single characters can be rendered in one (e.g., "1"), two (e.g., "J") or three operations (e.g., "P"). The number had a height of 12 mm and a width of 14 mm. (3 operations)
- (2) 2x2 grid of toggles, with two filled and two unfilled, covering a 17x17 mm area. (4 operations)
- (3) 3 sliders, partially filled at 10%, 50%, and 90%, respectively. The sliders were rendered over a 28x16 mm area. (5 operations)

- (4) The text "GOOD LIFE" represents our ability to render 7-segment strings of arbitrary length using at most five operations. The text was rendered over a 28x8 mm area. (5 operations)

The brightness was measured using the previously described experimental procedure, but we focused our comparison on parallel PMOLED (this work) and the best-performing baseline, the 5.5" AMOLED display (baseline 3).

The parallel PMOLED rendering was brighter than the AMOLED for all materials and shapes, except the basswood sheet, as seen in Figure 14 and the table in Appendix C. For both displays, the 1.6 mm basswood sheet did not let more than 4 lux pass through, which is far below the comfortable legibility of 31 lux for indoor display [20]. For all other materials, we observed a 3.6–9.3X brightness increase for parallel rendering. Across all conditions, except the light-blocking basswood, parallel rendering was 5–8.7X brighter for the text "2", 5.7–9.3X brighter for the 4 toggles, 4.9–6X brighter for the 3 sliders, and 3.6–7.2X brighter for the text "GOOD LIFE". Therefore, with a larger number of operations and more complex shapes, parallel PMOLED rendering is still significantly brighter than the best-performing AMOLED display.

### 7.4 Discussion

The technical evaluation suggests that parallel PMOLED rendering can enable hidden interfaces using a wide range of everyday materials, such as acrylic, PETG, wood veneer, mirror and textile. While the thick basswood sheet (1.6 mm) was not sufficiently transmissive, the thinner wood veneer (0.5 mm) worked well. For the compatible materials, we observed a significant advantage for parallel PMOLED rendering both for primitives (small/large, filled/unfilled rectangles) and for representative UI elements. For the primitives, we observed an improvement of at least 5X and in some cases exceeding 40X over the baselines. For the representative UI elements, we observed an improvement of between 3.6–9.3X over the best-performing AMOLED. It is encouraging that content-adaptive display driving can make effective use of low-resolution, low-complexity PMOLED displays. At the cost of around \$2.5 in large quantities [1], they are

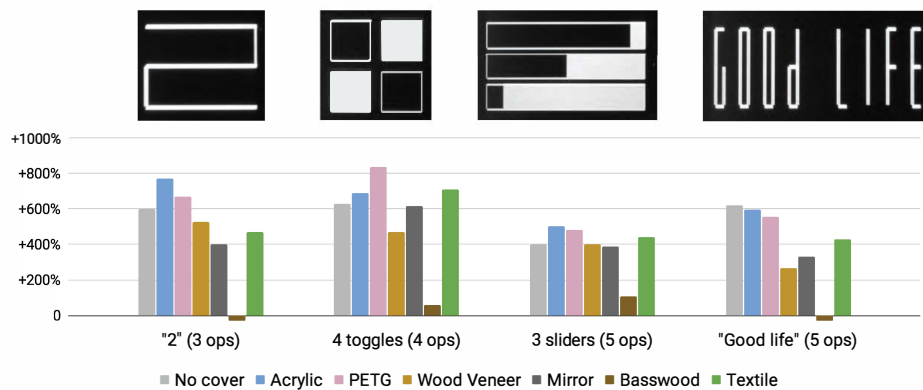


**Figure 14: Brightness experiment with representative shapes.** Measurements are done across seven material conditions using PMOLED parallel (this work) and large state-of-the-art AMOLED display. Photos of the shapes (f/22, 1/5s, ISO100, and 420 lx) are shown above the measurement plots.

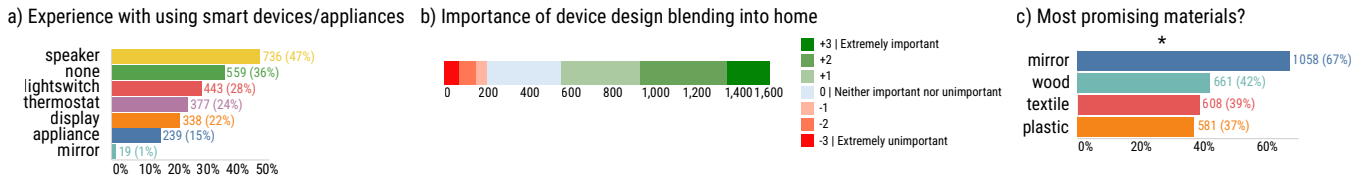


Figure 15: a) Participants’ experience with different smart appliances or devices (they could select more than one). b) Distribution of participants who rated how important it was that smart device design matched the style of the home. c) Mirror was considered the most promising material for hidden interfaces (participants could choose more than one).



Figure 16: Left: Distribution of desirability ratings for the six proposed use cases based on images and a video that participants watched (see supplementary material). Right: Images shown in the survey to ask participants about the desirability for each use case after having watched a video with interactive versions of these UIs. Each image shows a home device scenario and a closeup of the UI on our display under the corresponding material.

a viable and practical opportunity for ubiquitous devices, compared to popular high-fidelity AMOLEDs, which are significantly more expensive (\$24.50 in large quantities over 1000 [31]).

These findings suggest that parallel rendering on PMOLED has the potential for significantly better performance to enable hidden interfaces in everyday materials, at a lower cost than competing alternatives and without drastically increasing power consumption.

## 8 FEEDBACK ON IMPLEMENTED USE CASES WITH 1572 PARTICIPANTS

The foundational surveys asked participants to *imagine* hidden display scenarios, helping inform our implementation. In this survey we use *video and photos of our interactive UI prototypes* to solicit initial feedback on potential desirability.

### 8.1 Participants

We leveraged Google Surveys [11] again to deploy a nine-question survey to Android users of the Google Opinion Rewards app (requirement when using video), and we targeted the general population in the United States of all ages and gender. Figure 15a) and b) summarize participants’ experience with smart devices/appliances, and perceived importance of device style and aesthetics. Of the 1572 responses 45% were women and 55% men, across all age ranges (18%: 18–24, 25%: 25–34, 21%: 35–44, 14%: 45–54, 10%: 55–64, and 12% were 65+).

### 8.2 Results

After answering background questions, participants watched a one-minute video with different possibilities for creating interactive

graphical displays that could appear through four chosen materials (wood, mirror, textile and plastic). We summarize the main findings in this section, but the detailed results from the statistical analysis are provided in Appendix B.

*Use cases.* For six use cases, we showed participants an image (limited by the platform to 300×250 pixels) of an appliance in a home context next to a closeup of a UI on our display under the corresponding material (See Figure 16). Respondents ranked the desirability of each use case on a 5-point Likert scale. The analysis shows that the mirror use case was rated significantly higher than the thermostat, furniture and lightswitch use cases (See Figure 16). The lightswitch use case was also significantly lower rated than mirror, appliance and speaker.

*Most promising material.* We also asked participants which traditional materials they found to be the most promising for hiding displays. Results are summarized in Figure 15c, showing that mirror was rated as significantly more promising than the other materials, and that wood was rated significantly higher than plastic.

### 8.3 Discussion

*The smart mirror was considered the most promising use case and material.* The foundational surveys identified general interest in mirror materials, but its popularity really stood out in this survey. While only 19/1572 participants ( $\approx 1\%$ ) had experience with smart mirrors, 1058 (67%) identified mirror as one of the most promising materials, and it was consistently ranked as the most desirable use case. The ubiquity of mirrors in homes, combined with a clearer image quality as compared to the three diffusing materials, might have contributed to the positive rankings. Further research is needed for further qualitative insights.

*Information display use cases seemed to be more preferred than tangible controls.* The results suggest that information display use cases may be more promising for hidden interfaces. We showed a progress bar on a dishwasher, a visual alert on a smart mirror and sound visualization on a smart speaker. In contrast, the lightswitch was consistently ranked lowest, followed by thermostat and furniture controls. Users may prefer the tangible benefits of physical controls, for example, when finding the switch to turn on the lights in a dark room. Users might also already have accepted how devices are installed and used in the home, being more reluctant to modifications to walls and furniture in contrast to devices and appliances. Further research and studies are needed.

## 9 USER STUDY

The large-scale surveys provided a large-scale perspective on the motivation for our use cases with thousands of respondents with diverse backgrounds. Those results, combined with our technical evaluation, informed our interest in further insights from in-person participant feedback on content, materials and interactions with our prototype. We concluded that an in-person lab study would be well-suited to provide such complementary technical and qualitative feedback from hands-on user experience and impressions.

### 9.1 Participants

We recruited 11 participants in the US from a local university, three were women and eight were men. Two participants were 18-24, and nine were 25-34 years old (we only collect age ranges at our institution). The participants were students (5), engineers (4) and researchers (2), and received no compensation.

### 9.2 Apparatus

We used the display hardware prototype described in Section *Implementation* with Python software adapted for our user experiments. The display was positioned at a 27-degree-angle, 30 cm from the participant's eyes. An office lamp (LED bulb, 3000K) with a dimmer was used to adjust the lighting to reach desired levels, as measured by a light meter (SpeedmasterL-958D-U, Sekonic). The experiments used three levels: dark (3-5 lux), normal (80-100), and bright (180-200 lux). The experiments focused on the most promising materials from the large-scale surveys: wood veneer (#4, SCV-20-MXDOM&EXOTIC, Sauers, 0.5 mm) and mirror (#5, SV006901000, HIDBEA, 0.2 mm). Additionally, we included textile (#7, Gray Linen Fabric, Dekoth, 0.4 mm) given its popularity in smart speaker products.

### 9.3 Study design

*9.3.1 Legibility: possible and preferred content sizes under different material and lighting conditions.* This experiment shows content on the display to the participant, as it is covered by three different materials and under three different lighting conditions. The material and lighting condition orders were randomized. These preliminary experiments serve as an initial exploration of text visibility on our displays using our proof-of-concept character set.

- (1) *Minimum character size.* A random character (number or letter) was shown. The size was increased in steps by the experimenter until the participant could recognize and verbally

confirm the shown character. Each participant performed 90 trials (10 repetitions  $\times$  3 materials  $\times$  3 lighting conditions).

- (2) *Preferred UI sizes.* One of three UI elements was shown on the display (bar graph, toggle, three-letter string). The experimenter adjusted the content size until the participant said it was their preferred size. Each participant performed 27 trials (3 content types  $\times$  3 materials  $\times$  3 lighting conditions).

*9.3.2 Interacting with a hidden interface.* This experiment uses a more realistic hidden interface for interaction with contents under the mirror material, which was the highest rated in our large-scale surveys. Participants were asked to match a prompted target temperature by increasing/decreasing a simulated thermostat control using touch, while monitoring corresponding changes of displayed digits and a bar chart. The target value was randomized to 10–20 steps below/above the current value and participants performed 10 trials under normal lighting. We were primarily interested in giving participants an informed experience for our qualitative feedback form, although we measured performance to understand how the experience varied across participants. Therefore, we did not include a baseline, given that our emphasis was not on how well our touch interface performed.

*9.3.3 Qualitative feedback: Feedback form.* Participants filled out an extended form that combined questions from the three large-scale surveys. In addition to the questions and viewing the video with the concepts, they were also able to provide more detailed open-ended feedback.

## 9.4 Analysis

We performed repeated measures analysis of variance (ANOVA) and pair-wise post-hoc comparisons using paired samples t-tests with Bonferroni correction for the legibility and interaction tasks. For the surveys, similarly to the large-scale survey analysis, we performed KW tests and pair-wise post-hoc comparisons using MWU with Bonferroni correction.

## 9.5 Legibility and interaction

*9.5.1 Legibility: minimum character size.* ANOVAs for each of the three brightness levels suggested a significant effect of material on character size ( $F_{dark}(2, 20)=159.77$ ,  $F_{normal}(2, 20)=153.89$ ,  $F_{bright}(2, 20)=192.00$ , all  $P<.001$ ). Post-hoc analyses suggest that mirror ( $\bar{x}_{dark}=8.26$ ,  $\bar{x}_{normal}=8.35$ ,  $\bar{x}_{bright}=8.79$ ) allowed a significantly smaller character size (all  $P<.001$ ), whereas no effect was found between textile ( $\bar{x}_{dark}=20.76$ ,  $\bar{x}_{normal}=20.82$ ,  $\bar{x}_{bright}=21.84$ ) and wood ( $\bar{x}_{dark}=20.20$ ,  $\bar{x}_{normal}=21.45$ ,  $\bar{x}_{bright}=21.75$ ). ANOVAs for each of the materials suggested an effect of brightness on minimum character size for wood ( $F_{wood}(2, 20)=3.91$ ,  $P=.04$ ), although that effect was not present in the post-hoc analyses. No effect was seen for mirror ( $F_{mirror}(2, 20)=0.71$ ,  $P=.50$ ) or textile ( $F_{textile}(2, 20)=1.98$ ,  $P=.16$ ). See Figure 17, left and Table 3, left.

*9.5.2 Legibility: Character error rate.* Occasionally, the characters were identified incorrectly. Overall error rate was 2.93%. The letter 'g' had the highest error with 6 misidentifications, followed by 'd' (4 errors), and 'e', 'a' and '8' with 3 errors. Letter 'q' was misclassified twice, and 'p, y, 9, 7, s, n' once. Wood and textile had 14 and 12 misidentification errors, respectively, while the mirror material had

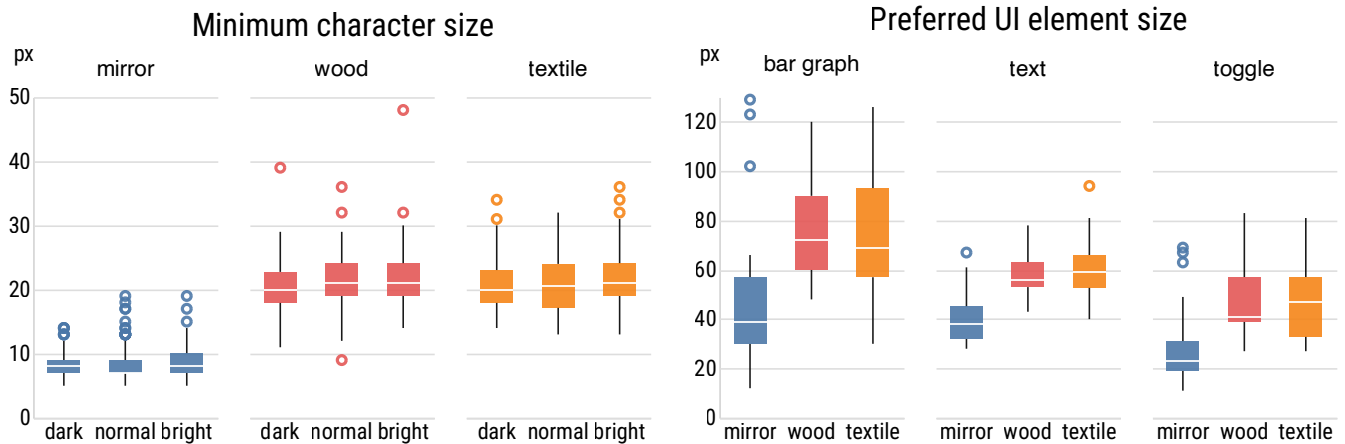


Figure 17: Legibility experiments for the three materials (mirror, wood, textile), grouped by the three environmental lighting conditions (dark, normal, bright). *Left*: Distribution of minimum character sizes (10 repetitions per condition). *Right*: Distribution of preferred character sizes for bar graph, text (three-letter string), and toggle.

Table 3: Effect of material on minimum character size and preferred UI element sizes. ANOVAs and paired samples t-tests show that the mirror material enabled significantly smaller sizes than textile or wood materials. (\*\*\*:  $P < .001$ , \*\*:  $P < .005$ , \*:  $P < .05$ )

	Minimum character size			Preferred UI element size		
	dark	normal	bright	dark	normal	bright
$F(2, 20)$	159.77	153.89	192.00	35.98	60.93	41.27
$t_{textile/mirror}(10)$	***16.10	***17.51	***16.19	***6.86	***10.05	***7.32
$t_{textile/wood}(10)$	0.59	-0.67	0.10	0.32	-0.64	1.30
$t_{mirror/wood}(10)$	***-19.60	***-15.20	***-18.76	***-8.88	***-8.82	***-6.93

only 3 errors. The number of errors did not differ significantly due to brightness level, with 7 errors made in low brightness and 11 in both normal and high brightness.

**9.5.3 Legibility: Preferred UI element size.** ANOVAs for each of the three brightness levels suggest a significant effect of material on preferred UI element size for the bar graph, toggle and the 3-letter text string ( $F_{dark}(2, 20)=35.98$ ,  $F_{normal}(2, 20)=60.93$ ,  $F_{bright}(2, 20)=41.27$ , all  $P < .001$ ). We observed a similar effect as for the minimum character size, as also these post-hoc analyses suggested that mirror ( $\bar{x}_{dark}=36.79$ ,  $\bar{x}_{normal}=37.85$ ,  $\bar{x}_{bright}=40.48$ ) resulted in a significantly smaller preferred element size (all  $P < .001$ ), while no effect was found between textile ( $\bar{x}_{dark}=61.70$ ,  $\bar{x}_{normal}=58.91$ ,  $\bar{x}_{bright}=62.85$ ) and wood ( $\bar{x}_{dark}=60.58$ ,  $\bar{x}_{normal}=60.30$ ,  $\bar{x}_{bright}=60.15$ ). ANOVAs for each of the materials did not show an effect of brightness on minimum character size for any material ( $F_{mirror}(2, 20)=2.70$ ,  $P=.09$ ;  $F_{wood}(2, 20)=0.02$ ,  $P=.98$ ;  $F_{textile}(2, 20)=1.85$ ,  $P=.18$ ). See Figure 17, right and Table 3, right.

**9.5.4 Interaction.** It took participants approximately 5 seconds on average ( $\bar{x}=4.98$ ,  $SD=1.74$ ) to increase/decrease the value by 10–20 steps. A step change took less than 0.5 seconds on average ( $\bar{x}=0.38$ ,  $SD=0.13$ ). We observed a 16% error rate where participants indicated

completion while their final value deviated from the target value by  $\pm 1$  (15/18),  $\pm 2$  (1/18), or  $\pm 3$  (2/18). Participants 4 and 10 represented more than half of the errors (10/18) with 6 and 4 errors, respectively. Figure 18 also suggests that participant 4 was distinctly slower than other participants.

## 9.6 Survey and ratings

All participants had experience with a smart home device and they all found it desirable that device aesthetics matched the existing style in their homes. Most of our participants (9/11) also found it desirable that displays and devices could appear on-demand.

**9.6.1 Material preferences.** A KW test found a significant effect for how participants rated material desirability ( $H(3)=9.21$ ,  $P=.03$ ), but that effect was not present in post-hoc analyses using MWU tests. The results from the user study do, however, align with the popularity of the mirror material in the large-scale survey. In fact, the average score for mirror was more than twice as high ( $\bar{x}=1.91$ ) compared to wood ( $\bar{x}=0.91$ ), plastic ( $\bar{x}=0.82$ ), and more than four times that of textile ( $\bar{x}=0.45$ ).

For the separate question on the most promising materials, where participants could select multiple materials, mirror was again the most popular (10/11), followed by wood (7/11), plastic (6/11) and

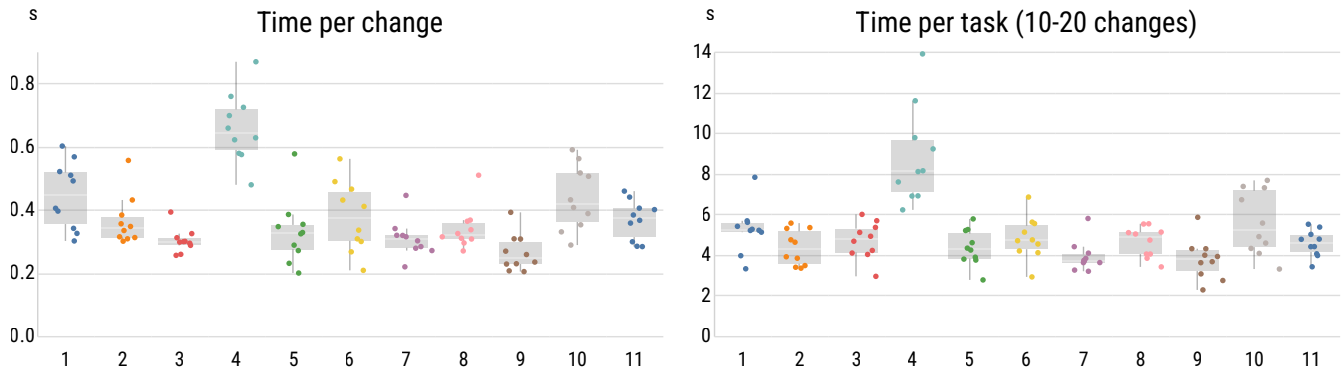


**Figure 18: Interacting with a simulated thermostat on the hidden display, time distributions for the 11 participants. Left: Time to make one step value change. Right: Overall task time of changing a value by  $\pm 10$ –20 steps.**

textile (5/11). A KW test did, however, not find a significant effect ( $H(3)=5.375$ ,  $P=.15$ ).

**9.6.2 Content preferences.** We ran a KW test for the desirability of the different content types, which revealed a significant effect ( $H(4)=25.62$ ,  $P<.001$ ). Posthoc analysis with MWU tests found significant differences when comparing basic content (text, input controls, icons) vs. image-based content (images/video); text vs. images/video ( $MWU_{text/images}=106$ ,  $P=.04$ ;  $MWU_{text/video}=105$ ,  $P=.04$ ), input controls vs. images/video ( $MWU_{controls/images}=10$ ,  $P=.01$ ;  $MWU_{controls/video}=11$ ,  $P=.02$ ), and icons vs. images/video ( $MWU_{icons/images}=108$ ,  $P=.02$ ;  $MWU_{icons/video}=107$ ,  $P=.03$ ). The analysis shows that text ( $\bar{x}=2.36$ ), input controls ( $\bar{x}=2.36$ ) and icons ( $\bar{x}=2.27$ ) were significantly higher rated than images ( $\bar{x}=0.36$ ) and video ( $\bar{x}=0.36$ ).

**9.6.3 Use case.** The average ratings for the different hidden interface use cases suggested that smart mirror was the most popular, although a KW test did not find a significant effect ( $H(5)=7.45$ ,  $P=.19$ ;  $\bar{x}_{mirror}=2.18$ ,  $\bar{x}_{appliance}=1.55$ ,  $\bar{x}_{speaker}=1.36$ ,  $\bar{x}_{thermostat}=1.36$ ,  $\bar{x}_{lightswitch}=1.27$ ,  $\bar{x}_{furniture}=1.18$ ).

## 9.7 Discussion

**9.7.1 Material affects minimum and preferred size of contents.** The results from the preliminary legibility experiment suggest that the material significantly affects the minimum character size and preferred UI element size. The mirror material enabled significantly smaller font sizes compared to wood or textile, since the mirror material diffuses less light, and characters appear more clear. That characteristic is also a plausible explanation for why participants were satisfied with smaller UI elements on the mirror material, while preferring larger ones with wood and textile. We observed no statistical significance difference between textile and wood.

Based on these findings, we see an opportunity for automatically adjusting rendering style and content size based on the cover material to maximize legibility, since we support scalable graphics and stroke thickness without sacrificing the high brightness.

We did not observe an effect of brightness levels on minimal character size or preferred UI element size, which might suggest

that the rectilinear rendering techniques perform similarly in dark and bright environments.

**9.7.2 Reducing the character misidentification errors.** Occasionally, characters were misidentified in the preliminary legibility experiment. It is not unlikely that material irregularities in the textile weave and wood grain could have been the cause of error. Occasionally such irregularities align with character strokes, interfering with their visibility. For example, 'q' was misclassified three times as 'c', due to not being able to clearly see the right vertical stroke. A possible solution is to have a completely uniform material; however, that might not be practical from a manufacturability, aesthetics or cost perspective. In the future, it may be interesting to explore strategies to dynamically shift the characters and/or adjust stroke weights. The movement could be minimal and imperceptible to the eye, which may alleviate blockages due to materials imperfections and non-uniformity. The scalable and dynamic nature of our display is a significant advantage over 7-segment and discrete LED displays, where shifting or stroke adjustment is not possible, making it challenging to compensate for irregular cover materials.

**9.7.3 Interactions with thermometer UI.** Our data suggests that most participants were able to successfully control the simulated thermometer with reasonable performance. These findings indicate that our prototype supports the exploration of intended ambient device scenarios where a hidden interface could appear on-demand for brief interactions. Upon discussion, the experimenter had observed that errors arose mainly from the capacitive touch sensing occasionally losing its calibration, which made it too, or not sufficiently, sensitive to the participant's touch. The sensitivity issues and a resulting slower performance was especially significant for participant 4.

**9.7.4 Qualitative in-person feedback.** The preferences and ratings by participants with hands-on device experience reinforced the feedback from 1572 survey respondents who had watched a video of the device and concept. The lab study confirmed the potential for mirror as the most promising material and the smart mirror as the highest rated use case. As in the evaluative large-scale survey, information display use cases (smart mirror, appliance, speaker) received higher

average scores than tangible controls (smart lightswitch, thermostat and furniture), even if those differences were not statistically significant for the 11 participants. Participants did, however, rate the importance of text, icons and input controls significantly higher than images and video. That feedback suggests that rectilinear rendering is well-suited for hidden interfaces, given its emphasis on simple vector-based UI graphics.

Participants also provided comments about the most positive and most negative aspects of the approach at the end of the study.

- **Seamlessness.** Participants appreciated the potential for seamless, integrated control of home devices: *"magical to make controls appear in walls or common objects [P4]", "can make control very convenient [P8]"*.
- **Appearance.** Another positive theme was related to appearance: *"makes every surface elegant [P8]", "would make certain objects appear more elegant [P4]", "simplicity [P10]", "aesthetics [P11]"*.
- **Discoverability.** Participants found discoverability both positive (*"guests [...] can't access my thermostat if they don't know where it is" [P6]*) and negative: *"difficult for people to understand the existence of interfaces [P11]", "invisibility might reduce the product functionality and our understanding of its functionality/existence [P5]"*.
- **Material interference.** Several participants expressed concerns with the diffusion of wood and textile: *"the dispersion of the light [P4]", "could be a hinder to user visibility [P7]", "not that clear behind some materials [P8]", "pattern [...] diffuses light [...] makes some numbers difficult to read [P9]"*.

## 10 LIMITATIONS AND FUTURE WORK

Our technique targets simple UIs that can be represented with rectilinear graphics. By leveraging parallel rendering, we demonstrate very bright displays that can project through materials. The use of rectilinear primitives, however, limits possible content and constrains the UI to a specific design aesthetic. While we show how typography can be efficiently represented using segmented rendering with significantly more expressivity than fixed 7-segment LED displays, we are also interested in representations of more general text, fonts and images. At that stage and with a more fully developed character set, we would be interested in end-to-end psychophysical evaluations of typeface properties, materials and visibility using more advanced methods, such as visual search tasks and adaptive staircase procedures [10, 36].

Future work could also investigate more advanced decompositions of vector graphics and natural images. Additionally, we observe that increased UI complexity adds operations, which reduce the overall brightness. For UIs where different screens have different complexity, consistent application brightness will require additional considerations, such as using global minimal brightness levels. Longitudinal deployments will complement the results from our large-scale surveys and lab evaluations by allowing us to go deeper into understanding user adoption and behavior with hidden interfaces.

In future work, we are also interested in exploring the technique on larger displays and with capacitive touch sensing overlaid on the

display, instead of around it. While the proof-of-concept implementation that we use is based on a large array of DACs, more efficient designs could be engineered based on FPGAs (field programmable gate arrays) or ASICs (application specific integrated circuit). Such designs would significantly reduce the size and the cost of the architecture, and would enable simple serial or I<sup>2</sup>C communication from basic microcontrollers.

Our large-scale surveys targeted the US since it was the largest population that we could deploy to with the survey tool. Additionally, the US has the highest penetration of smart home devices, which helped us get a large number of respondents with relevant experience. However, in the future, it will be helpful to expand to other geographical regions to understand how our results would apply to other populations.

## 11 CONCLUSION

In this work, we enable interfaces that can be embedded in traditional materials and appear on demand. Our large-scale online surveys and lab evaluation suggest unmet opportunities to introduce hidden displays with simple, yet expressive, dynamic and interactive UI elements and text in traditional materials, especially leveraging wood and mirror materials to blend into people's homes.

*Hidden Interfaces* leverages parallel rendering of rectilinear UIs to enable the significant brightness necessary to project through the materials that we use to hide the display. The low-complexity optimization of widely available PMOLED displays makes our approach particularly suitable for ubiquitous and ambient computing, where scalability and cost are critical considerations. The technique does not require display modifications, as it can be straightforwardly implemented in a modified display driver integrated circuit.

We present an interactive hardware system to implement hidden interfaces in different materials, such as wood veneer, plastics, textiles, and mirrors. We leverage our prototypes in technical characterization of the technique's abilities to project high-brightness visuals through a range of transmissive materials. The technical evaluation suggests that our technique can render rectilinear graphics with a significantly higher brightness than what is possible with both traditional scanline rendering and modern AMOLED displays. In most cases, our technique achieved a brightness improvement of >5–40X for primitives and 3.6X–9.3X for representative UI elements across different materials. It is particularly encouraging that our technical results suggest that we can meet our surveys' and lab study's interests in design-friendly materials such as wood veneer (>3–20X brightness) and mirrors (>4–40X brightness). We acknowledge that our technique is not general-purpose, but at 10% of the cost of comparable AMOLED and with unique brightness that allows simple graphics to penetrate wood veneer, mirrors, textile and plastic, we believe that it unlocks unique opportunities for ubiquitous computing.

The evaluative large-scale survey with 1572 participants, who viewed images and videos of our prototypes, provides further support for the potential of our implemented interfaces — especially the strong interest for smart mirror use cases and materials — which was further reinforced by an in-person lab study with 11 participants. The lab study also helped us characterize performance, indicating that parallel rendering is effective across different materials

(wood, textile, and mirror) and lighting conditions. We found that materials impacted the minimum viewable character size, where mirror materials enabling a significantly smaller size than wood or textile.

*Hidden Interfaces* demonstrates how control and feedback surfaces of smart devices and appliances could disappear when not in use, and appear on the user's proximity or touch. We hope that this direction will inspire the community to consider other approaches and scenarios where technology can fade into the background for a more harmonious coexistence with traditional materials and human environments.

## ACKNOWLEDGMENTS

First and foremost, we would like to thank Ali Rahimi and Roman Lewkow for the collaboration, including providing the enabling technology. We also thank Olivier Bau, Aaron Soloway, Mayur Panchal and Sukhraj Hothi for their prototyping and fabrication contributions. We thank Michelle Chang and Mark Zarich for visual designs, illustrations and presentation support. We thank Google ATAP and the Google Interaction Lab for their support of the project. Finally, we thank Sarah Sterman and Mathieu Le Goc for valuable discussions and suggestions, and our reviewers for their useful feedback and perspectives.

## REFERENCES

- [1] Ltd. Beihai Nutec Technology Co. 2022. 1.32 inch OLED display screen monochrome white with 128\*96 25PIN. [https://www.alibaba.com/product-detail/OLED-1-3-Inch-128x96-White\\_62531018562.html](https://www.alibaba.com/product-detail/OLED-1-3-Inch-128x96-White_62531018562.html). Accessed 2022-03-22.
- [2] Oliver Bimber and Daisuke Iwai. 2008. Superimposing Dynamic Range. *ACM Trans. Graph.* 27, 5, Article 150 (Dec. 2008), 8 pages. <https://doi.org/10.1145/1409060.1409103>
- [3] Leah Buechley, Mike Eisenberg, Jaime Catchen, and Ali Crockett. 2008. The LilyPad Arduino: Using Computational Textiles to Investigate Engagement, Aesthetics, and Diversity in Computer Science Education. In *Proceedings of the SIGCHI Conference on Human Factors in Computing Systems* (Florence, Italy) (CHI '08). Association for Computing Machinery, New York, NY, USA, 423–432. <https://doi.org/10.1145/1357054.1357123>
- [4] Byecold. 2022. Wifi multifunction bathroom smart mirror. [https://www.byecold.com/light\\_and\\_heated\\_mirrors/](https://www.byecold.com/light_and_heated_mirrors/). Accessed 2022-03-22.
- [5] Kunigunde Cherenack, Christoph Zysset, Thomas Kinkeldei, Niko Müntenrieder, and Gerhard Tröster. 2010. Woven electronic fibers with sensing and display functions for smart textiles. *Advanced materials* 22, 45 (2010), 5178–5182.
- [6] Artem Dementyev, Jeremy Gummeson, Derek Thrasher, Aaron Parks, Deepak Ganesan, Joshua R. Smith, and Alanson P. Sample. 2013. Wirelessly Powered Bistable Display Tags. In *Proceedings of the 2013 ACM International Joint Conference on Pervasive and Ubiquitous Computing* (Zurich, Switzerland) (UbiComp '13). Association for Computing Machinery, New York, NY, USA, 383–386. <https://doi.org/10.1145/2493432.2493516>
- [7] Laura Devendorf, Joanne Lo, Noura Howell, Jung Lin Lee, Nan-Wei Gong, M. Emre Karagozler, Shihou Fukuhara, Ivan Poupyrev, Eric Paulos, and Kimiko Ryokai. 2016. "I Don't Want to Wear a Screen": Probing Perceptions of and Possibilities for Dynamic Displays on Clothing. In *Proceedings of the 2016 CHI Conference on Human Factors in Computing Systems* (San Jose, California, USA) (CHI '16). Association for Computing Machinery, New York, NY, USA, 6028–6039. <https://doi.org/10.1145/2858036.2858192>
- [8] Christine Dierk, Molly Jane Pearce Nicholas, and Eric Paulos. 2018. AlterWear: Battery-Free Wearable Displays for Opportunistic Interactions. In *Proceedings of the 2018 CHI Conference on Human Factors in Computing Systems* (Montreal QC, Canada) (CHI '18). Association for Computing Machinery, New York, NY, USA, 1–11. <https://doi.org/10.1145/3173574.3173794>
- [9] Christine Dierk, Tomás Vega Gálvez, and Eric Paulos. 2017. AlterNail: Ambient, Batteryless, Stateful, Dynamic Displays at Your Fingertips. In *Proceedings of the 2017 CHI Conference on Human Factors in Computing Systems* (Denver, Colorado, USA) (CHI '17). Association for Computing Machinery, New York, NY, USA, 6754–6759. <https://doi.org/10.1145/3025453.3025924>
- [10] Jonathan Dobres, Nadine Chahine, Bryan Reimer, David Gould, Bruce Mehler, and Joseph F Coughlin. 2016. Utilising psychophysical techniques to investigate the effects of age, typeface design, size and display polarity on glance legibility. *Ergonomics* 59, 10 (2016), 1377–1391.
- [11] Google. 2018. Google Surveys Methodology. [http://services.google.com/fh/files/misc/white\\_paper\\_how\\_google\\_surveys\\_works.pdf](http://services.google.com/fh/files/misc/white_paper_how_google_surveys_works.pdf). Accessed 2022-03-22.
- [12] Google. 2022. Nest Mini. [https://store.google.com/us/product/google\\_nest\\_mini](https://store.google.com/us/product/google_nest_mini). Accessed 2022-03-22.
- [13] Google. 2022. Nest Thermostat E. [https://store.google.com/product/nest\\_thermostat\\_e](https://store.google.com/product/nest_thermostat_e). Accessed 2022-03-22.
- [14] Google. 2022. Thermostats. <https://nest.com/>. Accessed 2022-03-22.
- [15] Bin Hu, Dapeng Li, Okan Ala, Prakash Manandhar, Qinguo Fan, Dayalan Kasilingam, and Paul D Calvert. 2011. Textile-Based Flexible Electroluminescent Devices. *Advanced Functional Materials* 21, 2 (2011), 305–311.
- [16] Curiouser Products Inc. 2022. The Mirror. <https://www.mirror.co/>. Accessed 2022-03-22.
- [17] Hiroshi Ishii and Brygg Ullmer. 1997. Tangible Bits: Towards Seamless Interfaces between People, Bits and Atoms. In *Proceedings of the ACM SIGCHI Conference on Human Factors in Computing Systems* (Atlanta, Georgia, USA) (CHI '97). Association for Computing Machinery, New York, NY, USA, 234–241. <https://doi.org/10.1145/258549.258715>
- [18] Lasse Kaila, Henrik Raula, Miika Valttonen, and Karri Palovuori. 2012. Living Wood: A Self-Hiding Calm User Interface. In *Proceeding of the 16th International Academic MindTrek Conference* (Tampere, Finland) (MindTrek '12). Association for Computing Machinery, New York, NY, USA, 267–274. <https://doi.org/10.1145/2393132.2393191>
- [19] Douglas Lanman, Gordon Wetzstein, Matthew Hirsch, Wolfgang Heidrich, and Ramesh Raskar. 2011. Polarization Fields: Dynamic Light Field Display Using Multi-Layer LCDs. In *Proceedings of the 2011 SIGGRAPH Asia Conference* (Hong Kong, China) (SA '11). Association for Computing Machinery, New York, NY, USA, Article 186, 10 pages. <https://doi.org/10.1145/2024156.2024220>
- [20] Po-Hung Lin and Wen-Hung Kuo. 2011. Image quality of a mobile display under different illuminations. *Perceptual and motor skills* 113, 1 (2011), 215–228.
- [21] Jennifer Mankoff, Anind K. Dey, Gary Hsieh, Julie Kientz, Scott Lederer, and Morgan Ames. 2003. Heuristic Evaluation of Ambient Displays. In *Proceedings of the SIGCHI Conference on Human Factors in Computing Systems* (Ft. Lauderdale, Florida, USA) (CHI '03). Association for Computing Machinery, New York, NY, USA, 169–176. <https://doi.org/10.1145/642611.642642>
- [22] Benjamin Medvitz. 2016. Challenges for Outdoor Digital Displays. *Information Display* 32, 3 (2016), 38–42.
- [23] Shree K. Nayar, Peter N. Belhumeur, and Terry E. Boult. 2004. Lighting Sensitive Display. *ACM Trans. Graph.* 23, 4 (Oct. 2004), 963–979. <https://doi.org/10.1145/1027411.1027414>
- [24] Simon Olberding, Michael Wessely, and Jürgen Steimle. 2014. PrintScreen: Fabricating Highly Customizable Thin-Film Touch-Displays. In *Proceedings of the 27th Annual ACM Symposium on User Interface Software and Technology* (Honolulu, Hawaii, USA) (UIST '14). Association for Computing Machinery, New York, NY, USA, 281–290. <https://doi.org/10.1145/2642918.2647413>
- [25] Alex Olwal, Jon Moeller, Greg Priest-Dorman, Thad Starner, and Ben Carroll. 2018. I/O Braid: Scalable Touch-Sensitive Lighted Cords Using Spiraling, Repeating Sensing Textiles and Fiber Optics. In *Proceedings of the 31st Annual ACM Symposium on User Interface Software and Technology* (Berlin, Germany) (UIST '18). Association for Computing Machinery, New York, NY, USA, 485–497. <https://doi.org/10.1145/3242587.3242638>
- [26] Linda Oscarsson, Elisabeth Jacobsen Heimdahl, Torbjörn Lundell, and Joel Peterson. 2009. Flat knitting of a light emitting textile with optical fibres. *Autex Research Journal* 9, 2 (2009), 61–65.
- [27] Roshan Lalitha Peiris, Owen Noel Newton Fernando, and Adrian David Cheok. 2011. Flexible, Non-Emissive Textile Display. In *Proceedings of the Second International Conference on Ambient Intelligence* (Amsterdam, The Netherlands) (Aml'11). Springer-Verlag, Berlin, Heidelberg, 167–171. [https://doi.org/10.1007/978-3-642-25167-2\\_20](https://doi.org/10.1007/978-3-642-25167-2_20)
- [28] Reflectel. 2022. MIRROR TV. <https://reflectel.com/mirror-tv/>. Accessed 2022-03-22.
- [29] Seura. 2022. Séura TV Mirrors. <https://www.seura.com/products/tv-mirrors/>. Accessed 2022-03-22.
- [30] Chih-Tsung Shen, Zongqing Lu, Yi-Ping Hung, and Soo-Chang Pei. 2016. Visual Enhancement Using Sparsity-Based Image Decomposition for Low Backlight Displays. In *2016 IEEE International Symposium on Circuits and Systems (ISCAS)* (Montreal, QC, Canada). IEEE Press, New York, NY, USA, 2563–2566. <https://doi.org/10.1109/ISCAS.2016.7539116>
- [31] Ltd Shenzhen Topfoison Electronic Technology Co. 2022. 5.5 inch AMOLED Display 1080x1920 with mipi 4 lanes Oled Touch Screen Display. [https://www.alibaba.com/product-detail/Super-Thin-5-5-inch-1080P\\_62562430123.html](https://www.alibaba.com/product-detail/Super-Thin-5-5-inch-1080P_62562430123.html). Accessed 2022-03-22.
- [32] Sony. 2022. SRS-XB43. <https://www.sony.com/electronics/wireless-speakers/srs-xb43>. Accessed 2022-03-22.
- [33] Srikanth Kirshnamachari Sridharan, Juan David Hincapié-Ramos, David R. Flatla, and Pourang Irani. 2013. Color Correction for Optical See-through Displays Using Display Color Profiles. In *Proceedings of the 19th ACM Symposium on*

- Virtual Reality Software and Technology* (Singapore) (VRST '13). Association for Computing Machinery, New York, NY, USA, 231–240. <https://doi.org/10.1145/2503713.2503716>
- [34] Statista. 2022. Smart Home penetration rate forecast for selected countries in the segment Control and Connectivity 2020. <https://www.statista.com/forecasts/483772/smart-home-penetration-rate-for-selected-countries-in-the-segment-control-and-connectivity>. Accessed 2022-03-22.
- [35] Harold Thimbleby. 2013. *Reasons to Question Seven Segment Displays*. Association for Computing Machinery, New York, NY, USA, 1431–1440. <https://doi.org/10.1145/2470654.2466190>
- [36] Jean-Luc Vinot and Sylvie Athenes. 2012. *Legible, Are You Sure? An Experimentation-Based Typographical Design in Safety-Critical Context*. Association for Computing Machinery, New York, NY, USA, 2287–2296. <https://doi.org/10.1145/2207676.2208387>
- [37] Daniel Vogel and Ravin Balakrishnan. 2004. Interactive Public Ambient Displays: Transitioning from Implicit to Explicit, Public to Personal, Interaction with Multiple Users. In *Proceedings of the 17th Annual ACM Symposium on User Interface Software and Technology* (Santa Fe, NM, USA) (UIST '04). Association for Computing Machinery, New York, NY, USA, 137–146. <https://doi.org/10.1145/1029632.1029656>
- [38] Akira Wakita and Midori Shibutani. 2006. Mosaic Textile: Wearable Ambient Display with Non-Emissive Color-Changing Modules. In *Proceedings of the 2006 ACM SIGCHI International Conference on Advances in Computer Entertainment Technology* (Hollywood, California, USA) (ACE '06). Association for Computing Machinery, New York, NY, USA, 48–es. <https://doi.org/10.1145/1178823.1178880>
- [39] Tan Kiat Wee and Rajesh Krishna Balan. 2012. Adaptive Display Power Management for OLED Displays. In *Proceedings of the First ACM International Workshop on Mobile Gaming* (Helsinki, Finland) (MobileGames '12). Association for Computing Machinery, New York, NY, USA, 25–30. <https://doi.org/10.1145/2342480.2342487>
- [40] Mark Weiser and John Seely Brown. 1996. Designing calm technology. *PowerGrid Journal* 1, 1 (1996), 75–85.
- [41] Withings. 2022. Thermo. <https://www.withings.com/us/en/thermo>. Accessed 2022-03-22.

## 12 APPENDIX A: STATISTICAL ANALYSIS FOR LARGE-SCALE FOUNDATIONAL SURVEYS

This section provides detailed results for the statistical analyses of the two surveys (n=1499 and n=1502) discussed in section 3.

We analyze statistical significance on the non-parametric dataset using Kruskal-Wallis H-tests (KW), and Mann-Whitney U-tests (MWU) for pair-wise post-hoc comparisons with Bonferroni correction. For many questions, we analyze how participants' positive (+), neutral (0) and negative (-) attitudes for an independent variable affected different dependent variables, but we always evaluate against the full Likert-scale range.

### 12.1 Specific materials. Desirability for devices hidden under plastic, wood, mirror or textile. (n=1499)

**12.1.1 Material ratings.** A KW test found no significant difference ( $H(3)=1.26, P=0.74$ ) between ratings for the four materials' desirability as hidden displays ( $\bar{x}_{mirror}=-0.00, \bar{x}_{plastic}=-0.04, \bar{x}_{textile}=-0.04, \bar{x}_{wood}=-0.03$ ).

**12.1.2 Materials  $\times$  Design preference ("How important is it that smart device aesthetics and design blend in or match the style of existing objects and furniture in your home?").** We performed a KW test for the three design preference groups on each of the four materials and found a significant effect for all — plastic ( $H(2)=14.15, P<.001, \bar{x}_-=-0.29, \bar{x}_0=-0.01, \bar{x}_+=0.05$ ), wood ( $H(2)=47.60, P<.001, \bar{x}_-=-0.39, \bar{x}_0=-0.04, \bar{x}_+=0.26$ ), textile ( $H(2)=6.86, P=.03, \bar{x}_-=-0.14, \bar{x}_0=-0.05, \bar{x}_+=0.05$ ), and mirror ( $H(2)=29.88, P<.001, \bar{x}_-=-0.36, \bar{x}_0=0.01, \bar{x}_+=0.21$ ). Post-hoc analysis did, however, not find any effect for textile. For plastic, The MW tests revealed a difference between negative ( $\bar{x}_-=-0.29$ ) and neutral ( $\bar{x}_0=-0.01$ ) participants ( $MW_{-/0} U=101604, P=.03$ ). Post-hoc analysis found differences between all design attitude groups for both wood ( $MW_{-/0} U=48504, P<.001; MW_{-/0} U=99162, P=.002; MW_{+/0} U=191452, P<.001$ ) and mirror ( $MW_{-/0} U=50918, P<.001; MW_{-/0} U=99933, P=.004; MW_{+/0} U=182925, P=.02$ ).

### 12.2 Specific content. Desirability for different content. (n=1502)

**12.2.1 Content ratings.** A KW test found a significant effect between the five content types ( $H(4)=19.55, P<.001, \bar{x}_{controls}=0.20, \bar{x}_{icons}=0.21, \bar{x}_{images}=0.22, \bar{x}_{text}=0.24, \bar{x}_{video}=0.04$ ).

Post-hoc analysis revealed a difference between text and video ( $MW_{text/video} U=1214948, P=.004$ ), and images and video ( $MW_{images/video} U=1203333, P=.03$ ).

**12.2.2 Content  $\times$  Home device usage ("Do you use or have used any of these devices?").** We ran a KW test for the two device groups on

each of the five content types. People who had used home devices found text ( $\bar{x}_{no}=0.05 < \bar{x}_{yes}=0.41$ ), controls ( $\bar{x}_{no}=0.04 < \bar{x}_{yes}=0.34$ ), and images ( $\bar{x}_{no}=0.06 < \bar{x}_{yes}=0.35$ ) more desirable, as revealed by the KW tests ( $H_{text}(1)=21.51, P<.001; H_{controls}(1)=17.30, P<.001; H_{images}(1)=3.19, P=.07$ ) and post-hoc analyses ( $MW_{text} U=316412, P<.001; MW_{controls} U=312420, P=.002; MW_{images} U=309232, P=.01$ ). No significant effect was found for video ( $H_{video}(1)=3.19, P=.07, \bar{x}_{no}=-0.03, \bar{x}_{yes}=0.10$ ). While the KW test found an effect for icons ( $H(1)=9.93, P=.002, \bar{x}_{no}=0.09, \bar{x}_{yes}=0.31$ ), post-hoc analysis did not ( $MW_{icons} U=304457, P=.09$ ).

## 13 APPENDIX B: STATISTICAL ANALYSIS FOR LARGE-SCALE EVALUATIVE SURVEY

This section provides detailed results for the statistical analysis of the survey (n=1572) discussed in section 8.

As previously, our analysis is based on Kruskal-Wallis H-tests (KW), and pair-wise post-hoc comparisons using Mann-Whitney U-tests (MWU) with Bonferroni correction.

### 13.1 Use cases: smart appliances, furniture, speakers, thermostat, mirrors, lightswitches

**13.1.1 Use case desirability ratings ("How desirable would it be to you if the use case had display/controls that could appear from underneath traditional materials?").** A KW test found a significant effect ( $H(5)=66.88, P<.001$ ) between ratings for the six use cases ( $\bar{x}_{mirror}=0.57, \bar{x}_{appliance}=0.48, \bar{x}_{speaker}=0.47, \bar{x}_{furniture}=0.36, \bar{x}_{thermostat}=0.35, \bar{x}_{lightswitch}=0.29$ ). Mirror was highest rated with post-hoc analysis suggesting a significant difference when compared to lightswitch ( $MWU_{mirror/lightswitch}=1401435, P<.001$ ), furniture ( $MWU_{furniture/mirror}=1091895, P<.001$ ), and thermostat ( $MWU_{thermostat/mirror}=1103193, P<.001$ ).

The lightswitch was ranked lowest and significantly lower than the mirror, appliance ( $MWU_{appliance/lightswitch}=1342393, P<.001$ ) and speaker ( $MWU_{speaker/lightswitch}=1337395, P=.001$ ).

### 13.2 Most promising material

A KW test identified a significant effect ( $H(3)=382.23, P<.001$ ) and post-hoc analysis revealed that mirror was rated as significantly more promising than other materials ( $MWU_{mirror/wood}=923550, MWU_{mirror/plastic}=860670, MWU_{mirror/textile}=881892$ , all  $P<.001$ ). Additionally, wood was rated significantly higher than plastic ( $MWU_{wood/plastic}=1298472, P=.02$ ).

## 14 APPENDIX C: EVALUATION 2 OF REPRESENTATIVE UI ELEMENTS

Table 4 provides detailed results for the brightness characterization with additional representative user interface elements as described in Section 7.3.

**Table 4: Brightness experiment with representative shapes. Measurements are done across seven materials using PMOLED parallel (this work) and a large state-of-the-art AMOLED display. The X times dimmer in comparison to this work is color-coded from low to high as yellow to red.**

All values in lx	4 checkboxes (4 ops)			3 progress bars (5 ops)			Text: "2" (3 ops)			Text: "Good life" (5 ops)		
	Parallel PMOLED	5.5" AMOLED	X times dimmer	Parallel PMOLED	5.5" AMOLED	X times dimmer	Parallel PMOLED	5.5" AMOLED	X times dimmer	Parallel PMOLED	5.5" AMOLED	X times dimmer
<b>No cover</b>	800.00	110.00	7.27	900.00	180.00	5.00	300.00	43.00	6.98	360.00	50.00	7.20
<b>Acrylic</b>	450.00	57.00	7.89	600.00	100.00	6.00	200.00	23.00	8.70	160.00	23.00	6.96
<b>PETG</b>	560.00	60.00	9.33	640.00	110.00	5.82	200.00	26.00	7.69	170.00	26.00	6.54
<b>Wood Veneer</b>	53.00	9.30	5.70	70.00	14.00	5.00	25.00	4.00	6.25	16.00	4.40	3.64
<b>Mirror</b>	150.00	21.00	7.14	170.00	35.00	4.86	50.00	10.00	5.00	43.00	10.00	4.30
<b>Basswood</b>	3.50	2.20	1.59	3.30	1.60	2.06	1.40	2.00	0.70	1.40	2.00	0.70
<b>Textile</b>	170.00	21.00	8.10	200.00	37.00	5.41	53.00	9.30	5.70	53.00	10.00	5.30